frontiers in Physics

ORIGINAL RESEARCH
published: 31 January 2022
doi: 10.3389/fphy.2021.754423

A Cryogenic Hydrogen Ribbon for Laser Driven Proton Acceleration at Hz-Level Repetition Rate

T. Chagovets[1], J. Viswanathan[2], M. Tryus[1], F. Grepl[1,3], A. Velyhan[1], S. Stancek[1,4], L. Giuffrida[1], F. Schillaci[1], J. Cupal[1,3], L. Koubikova[1], D. Garcia[2], J. Manzagol[2], P. Bonnay[2], F. Souris[2], D. Chatain[2], A. Girard[2] and D. Margarone[1,5]*

[1]ELI Beamlines Centre, Institute of Physics, CAS, Dolni Brezany, Czechia, [2]Université Grenoble Alpes, CEA IRIG-DSBT, Grenoble, France, [3]Faculty of Nuclear Sciences and Physical Engineering, Czech Technical University in Prague, Prague, Czechia, [4]Joint Laboratory of Optics of Palacky University, Institute of Physics of Academy of Sciences of the Czech Republic, Faculty of Science, Palacky University, Olomouc, Czechia, [5]Centre for Plasma Physics, School of Mathematics and Physics, Queen's University Belfast, Belfast, United Kingdom

We report on recent progress in deploying a continuous solid hydrogen ribbon as a debris-free and renewable laser-driven source of pure proton beams generated by a 30-fs laser with ~1-J laser energy focused on target at relativistic intensities of ~10^{19} W/cm^2 and repetition rate of 0.1 Hz. The stability of the ribbon position versus the laser interaction point and maximum repetition rate was tested up to 3.3 Hz. The acceleration of protons with cut-off energies up to 1.5 MeV is demonstrated using a 100-μm thick hydrogen ribbon as proof-of-principle capability of the relatively thick target delivery system. The laser-target geometry presented demonstrates an experimental technique that can potentially enables the operation of a laser–plasma source at Hz-level repetition rate.

Keywords: laser proton acceleration, laser plasma interaction, solid hydrogen target, high repetition rate, high repetition target

OPEN ACCESS

Edited by:
Joan J. Carvajal, University of Rovira i Virgili, Spain

Reviewed by:
Jaume Massons, University of Rovira i Virgili, Spain
Gabriele Cristoforetti, Consiglio Nazionale Delle Ricerche, Italy

****Correspondence:***
T. Chagovets
timofej.chagovets@eli-beams.eu

Specialty section:
This article was submitted to Interdisciplinary Physics, a section of the journal Frontiers in Physics

Received: *06 August 2021*
Accepted: *15 December 2021*
Published: *31 January 2022*

Citation:
Chagovets T, Viswanathan J, Tryus M, Grepl F, Velyhan A, Stancek S, Giuffrida L, Schillaci F, Cupal J, Koubikova L, Garcia D, Manzagol J, Bonnay P, Souris F, Chatain D, Girard A and Margarone D (2022) A Cryogenic Hydrogen Ribbon for Laser Driven Proton Acceleration at Hz-Level Repetition Rate. Front. Phys. 9:754423. doi: 10.3389/fphy.2021.754423

INTRODUCTION

Over the last decades, the rapid development of high peak power (0.1–1 PW), femtosecond laser systems with repetition rates (up to 10 Hz) [1–4] has triggered a rapid progress of new research fields such as laser-driven ion acceleration [5]. The most experimentally investigated scheme for laser-plasma based ion acceleration is known as target normal sheath acceleration (TNSA) [6]. The mechanism is based on the generation of high-energy electrons by the laser pulse on the front surface of the target, crossing the target volume and trying to escape into the vacuum from the backside, thus generating ultrahigh space charge fields. Consequently, the ions are pulled off the target surface by the escaping electron cloud and accelerated to tens of MeVs in a few micrometers. Typically, metallic and plastic foils with a thickness of 1–100 μm are used as targets. An ion source of this kind presents an exponentially decreasing energy spectrum, short bunch duration of a few picoseconds at the source, and thus can be used to deposit a very high dose rate on a user sample. This source peculiarity is beneficial for a range of applications as radiobiology for pre-clinical studies of alternative proton therapy approaches [7–9] and compact neutron generation [10–12]. On the other hand, high repetition rate operation is very challenging in terms of target fabrication, and for the delivery system itself, including positioning, alignment, and real-time target characterization. Several options are currently used by the specialized community: planar target holders, tape targets, and targets carried on strips and belts [13]. Recent progress in developing planar target systems includes the capability to deliver and refresh solid targets at a

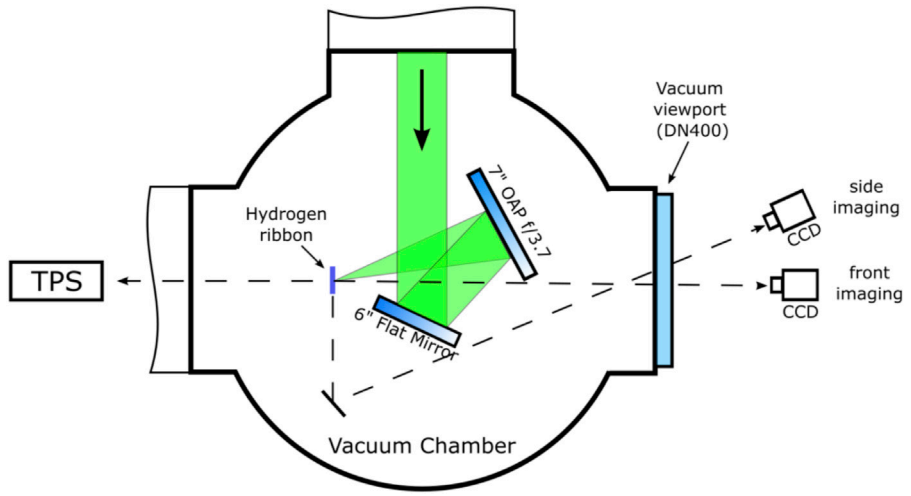

FIGURE 1 | Schematic view of the experimental setup in the interaction chamber (top view).

repetition rate up to 10 Hz, along with ion diagnostics, data acquisition, and real-time analysis methods [14]. However, there are certain drawbacks associated with the use of metallic or plastic targets. Target assemblies have to supply a high number of shots before the reloading process that typically requires to interrupt the experimental run due to the need to vent the vacuum chamber, align a new set of targets, and pump the chamber down before the following run. Additionally, increasing the laser peak power and repetition rate enhance the risk to contaminate sophisticated and expensive optics due to debris generation from the target (metallic or plastic foils). Currently, several approaches are being proposed and tested to address these technical issues. Recent developments span from the fabrication of liquid microjets [15, 16] to dense gas jets [17, 18], liquid crystal films [19, 20], and cryogenic microjets [21, 22]. The principal advantage of such target delivery systems is the ability to produce fresh targets for kHz laser operation; however, the resulting gas load can substantially increase the pressure inside the vacuum chamber, and thus becomes a clear limitation for ultrahigh intensity laser beam focusing and subsequent ion production.

The ELISE (Experiments on Laser Interaction with Solid hydrogEn) target delivery system designed and developed by the CEA team (Grenoble, France) provides an alternative approach to the production of a continuous flow of solid hydrogen [23]. This kind of target was successfully tested in previous experimental campaigns in single-shot laser mode at PALS (Czech Republic) [24] and at LULI (France) [25]. In this work, we report on recent progress in the operation of ELISE at high repetition rate and relativistic laser intensities and a proof-of-principle experiment of proton acceleration using the L3-HAPLS laser operating at the ELI Beamlines research center with the long-term goal of operating a proton source for user applications [26]. Target characterization, operation in high vacuum, and compatibility for Hz level repetition rate use are presented and discussed.

MATERIALS AND METHODS

The experiment was carried out at the TERESA (TEstbed for high REpetition-rate Sources of Accelerated particles) target area [27], which allows to utilize the circular sub-aperture (90 mm in diameter)of the L3-HAPLS laser with a reduced beam size of 90 mm (at $1/e^2$) in diameter, maximum pulse energy of 1.3 J on target, central wavelength of 810 nm, and duration of ~30 fs A scheme of the experimental setup is shown in **Figure 1**. An Off-Axis Parabola (OAP) with focal length of 330 mm (~f/3.7) allows to focus the beam down to a focal spot of 3.8 ± 0.1 μm in diameter. The angle of incidence on the target was adjusted to approximately 15°. The accelerated proton beam is measured in proximity of the target normal using a Thomson Parabola Spectrometer (TPS) at a distance of 2.15°m from the target. The TPS configuration is optimized for detection of protons in the energy range 0.1–5 MeV [28]. The second generation of ELISE target system relies on the use of a pulse-tube cryocooler as a cold source, removing the need of cryogenic fluids, which use can be cumbersome and expensive without an adequate helium recovery system. The ribbon production technique remains practically the same as described in [23]. The solidified hydrogen is pushed into the vacuum chamber through a dedicated nozzle, currently resulting in the continuous production of a solid hydrogen ribbon with a width of 1 mm and thickness of 75 μm or 100 μm, which can be extruded at different velocities.

Obviously, the stability of the target position during extrusion plays a key role for proton generation. The design of ELISE allows moving the cryostat only in the vertical direction, thus requires a focal position adjustment by fine movements of the OAP. This choice is dictated by the requirement to produce the ribbon continuously and minimize any significant manipulations during operations, hence to reduce vibrations. The solid hydrogen can experience some deformation after passing through the nozzle and this is an additional source of spatial fluctuations of the ribbon from the central extrusion axes that can prevent to reach

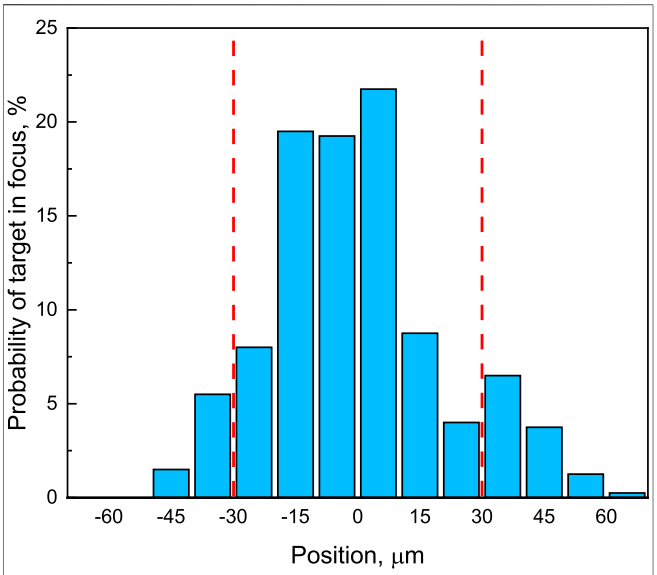

FIGURE 2 | Distribution of target position stability during a continuous acquisition. The ribbon is extruded using the 100-μm nozzle with an extrusion velocity of 3.1 mm/s. The red dash lines indicate the OAP Rayleigh range as boundaries of acceptable spatial jitter of the ribbon.

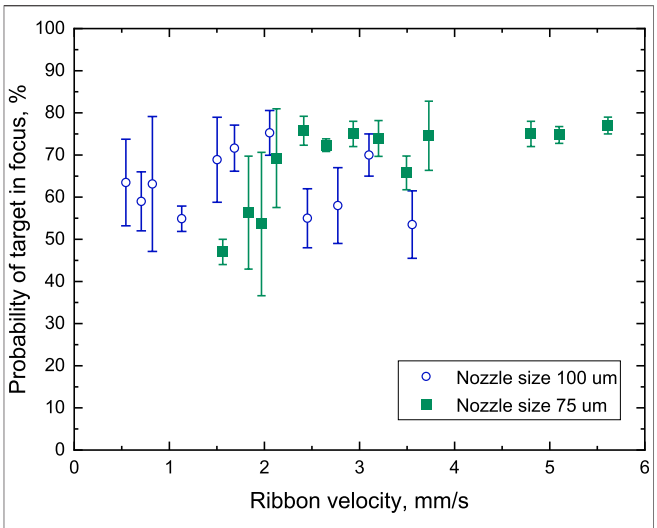

FIGURE 3 | Probability of the target position being in a ± 30 μm acceptable range as a function of target extrusion velocity for two nozzle sizes (the error bars denote the standard deviation of probability values obtained at a given ribbon velocity).

optimal conditions for laser-target interaction. In fact, single shot operation allows to carry out a manual adjustment of the position of the OAP after each shot. Additionally, various tools (rollers, cones, etc.) can be used to dynamically improve the stability of the ribbon position with respect to the focal plane, which is the region of highest laser intensity required for an optimal proton acceleration. However these manipulations are challenging when the laser operates at high-repetition-rate (>0.1 Hz).

To address these concerns, we characterized the target stability for different extrusion velocities. The displacement of the ribbon along the main laser axis was monitored by CCD cameras from two perpendicular views. A set of images for each extrusion velocity was acquired during 10°s operation at a rate of 40 FPS (frames per second). The use of a pixel-based image processing allowed to determine size, velocity, and spatial fluctuations of the ribbon, and to calculate the probability of the target to be located within the Rayleigh range of the laser beam waist.

The fluctuations in target thickness amounted to smaller than 10 μm and are ascribed to ribbon surface irregular structures caused by structural deformation of the polycrystalline solid hydrogen as it passes through the nozzle. Any displacement of the ribbon position in the direction perpendicular to the laser beam propagation is negligible with respect to the diameter of the focal spot, thus the laser pulse hits the target surface all the time. The situation is somewhat different in terms of stability in the laser propagation direction, which is the most critical requirement for an optimal laser-target interaction, hence proton acceleration. An example of ribbon deviation along the laser propagation axis is shown in **Figure 2**. The histogram represents the distribution of the ribbon position during acquisition at an extrusion velocity of about 3.1 mm/sec. A spatial jitter along the longitudinal (laser) axis was found taking into account a Rayleigh range of about ± 30 μm for this experimental setup. The resulting probability of the precise target positioning within the Rayleigh range as a function of extrusion velocity is shown in **Figure 3**. The error bars denote the standard deviation of probability values obtained for different runs at the corresponding ribbon velocity. These results revealed that more than 45% of laser shots remained focused on the target surface. All measurements were taken at a distance of 4 mm below the bottom edge of the nozzle; however, the amplitude of ribbon wobbling showed an increase with the distance from the nozzle. The operation time of ribbon extrusion is limited by a finite volume of the solid hydrogen pressure cell. The continuous operation time of the system during one full cooling cycle was tested with various ribbon extrusion velocity. For a ribbon speed of ~4 mm/s, the system could continuously operate over 6 h.

REPETITION RATE CAPABILITY

Of particular interest for future multidisciplinary applications of the accelerate proton beams is the maximum possible repetition rate of the laser that can be supported by the target. The time evolution of the target condition was investigated at two different laser intensities by means of optical probing as described above. In the first case, the ribbon was irradiated by the laser with a pulse energy of 300 mJ at 3.3 Hz repetition rate. **Figure 4** shows the ribbon condition during a sequence of 4 laser shots. After the laser absorption, the area of about ~0.6 mm in diameter is vaporized, while the rest of the ribbon body remains unperturbed. In this case, a ribbon speed of about 3 mm per second was enough to refresh the target.

For more energetic laser shots (>1 J) the destruction of the ribbon is more significant. **Figure 5** shows the condition of the ribbon before and after the shot. The ribbon is evaporated up to

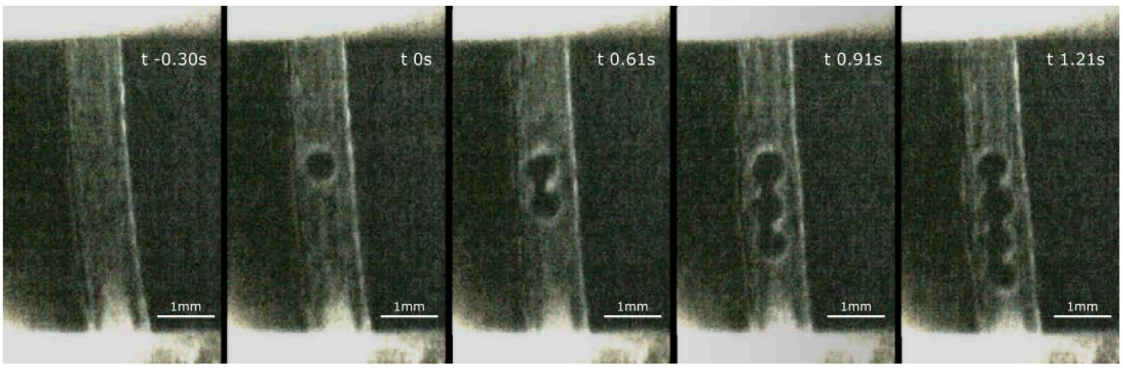

FIGURE 4 | Imaging of the ribbon extrusion using the 100-μm nozzle with a velocity of 3 mm/s during a sequence of 4 laser pulses with energy of 300 mJ (~1.5*10^{19} W/cm^2 intensity) at 3.3 Hz repetition rate. The left image shows the condition of the ribbon before the laser shot sequence. The images were taken 10 ms after each shot.

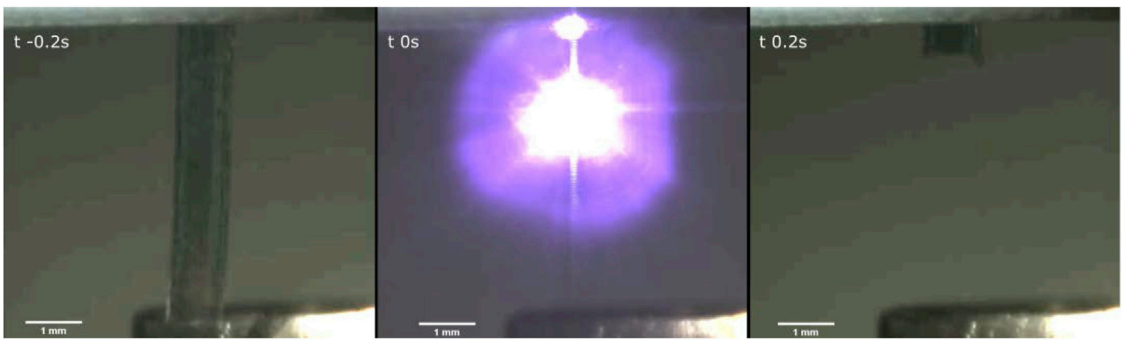

FIGURE 5 | Condition of the ribbon extruded at the velocity of 4 mm per second with 100-μm nozzle before (left) and after (right) irradiation with 1-J laser energy (~5*10^{19} W/cm^2 intensity) at 1 Hz repetition rate. The central image corresponds to an on-shot central view of the hydrogen ribbon.

~2 mm above the laser focal spot each shot; nevertheless, the destruction of the target does not affect the ribbon extrusion that proceeds with a constant velocity. Thus, a 1 Hz repetition rate is possible at 1-J energy level, however, higher repetition rate of the laser, or higher energies, would require an adequate target refreshing, thus a faster extrusion of the ribbon. As it will be discussed later, an increase of the target velocity causes a pressure rise in the vacuum chamber that also needs to be addressed.

VACUUM OPERATION WITH CONTINUOUSLY EXTRUDED SOLID RIBBON

Liquid and cryogenic target delivery systems are complex in terms of their implementation in a high vacuum environment and may require significant alteration of the vacuum system. Typically, continuous evaporation of the material during target production causes an additional gas load, which leads to pressure rise in the vacuum chamber. In fact, the background pressure is extremely important for laser propagation, ion acceleration, and smooth operation of the cryogenic equipment.

The behavior of the residual gas in the chamber can be described by two boundary conditions, which depend on the pressure in the vacuum chamber. These conditions can be determined from the kinetic theory of gases by the Knudsen number [29], $Kn = \lambda/L$, where λ is the mean free path and L is the characteristic length which can be taken as distance between the wall of the chamber and the target. In this case, the mean free path can be define from the gas kinetic theory as:

$$\lambda = \sqrt{\pi RT/(2M)} * \mu/p$$

where R is the gas constant, T is the temperature of the gas, M is the molecular mass, μ is the viscosity of the gas and p is its pressure (for more details see Ref. [30]).

At rough vacuum, for $Kn < 1$, the mean free path of the gas molecules is limited by collisions with other gas molecules. The collision of generated ions with residual gas can result in a significant reduction of the ion cut-off energy [16]. Furthermore, residual gas causes a dramatic heat transfer through the gas from the 'hot' surfaces of the chamber to the cold cryogenic parts [31]. At very low pressures (high vacuum),

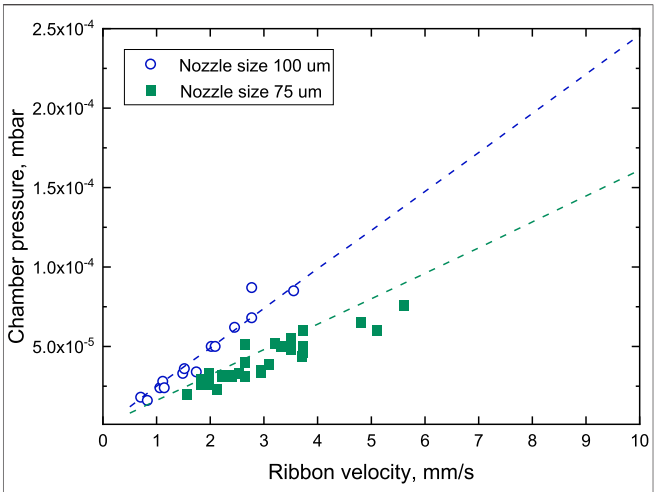

FIGURE 6 | Chamber pressure vs. ribbon extrusion velocity for two different nozzles (dash lines correspond to the theoretical estimation of the chamber pressure at different velocities of the ribbon for pumping capacity ~3500 L/s).

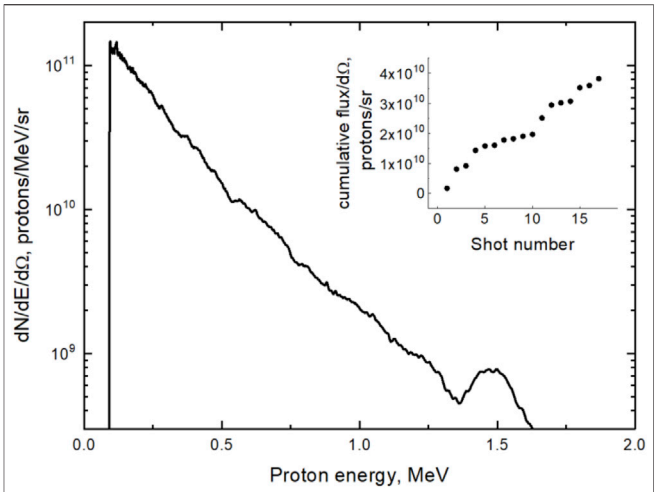

FIGURE 7 | Average proton energy distribution measured for the hydrogen targets (100 μm) in the target normal direction by the TPS. The inset shows the cumulative flux of the proton beam with energy range 0.2–1.5 MeV generated in 18 consecutive shots.

when $Kn > 1$, the mean free path of the molecules can become comparable to the distance between the chamber walls and the target, thus providing a longer scale length of gas density. A practical consideration is to keep the vacuum system in a free molecular regime where the accelerated ion beam propagates without interaction with the remnant gas molecules.

An estimate shows that the TERESA–ELISE system reaches the free molecular regime, $Kn > 1$, at a vacuum pressure below $1*10^{-4}$ mbar. The equilibrium pressure is therefore directly given by the mass flow through the nozzle divided by the pumping capacity of the TERESA vacuum system (about 3,500 L/s). **Figure 6** displays the measured chamber pressure as a function of the ribbon velocity. The calculated value of the equilibrium pressure is in good agreement with the measured ones in the current pumping speed setup (see **Figure 6**, dash lines). The current pumping ability of the TERESA vacuum system allows extruding the ribbon with maximum velocity of about 4 and 6 mm/s for 100-μm and 75-μm wide nozzles, respectively. This ribbon velocity is sufficient to satisfy laser operations at 3.3 Hz with moderate laser energies (<1 J). For higher laser energies, the ribbon velocity needs to be increased due to substantial destruction of the target after the shot. This limitation can be overcome by increasing the pumping ability of the vacuum system. Assuming that, a higher extrusion velocity of about 10 mm/s is needed to ensure target renewal at laser energies above 1 J and 3.3 Hz repetition rate. The corresponding gas load is needed to be covered by a pumping speed a factor of 3 higher than the one used in the current setup. This pumping speed can be reached by using additional turbomolecular pumps or adding a cryogenic pump with a pumping ability above 7,000 L/sec. However, keeping the same pumping system would only result in a reasonable pressure increase, as can be seen in **Figure 6**.

ION ACCELERATION

A modest performance of the proton source in terms of cutoff energy is expected due to the relatively large target thickness (~100 μm) and low energy of the laser pulse (<1 J). The increase of the laser energy above 1 J requires higher velocity of ribbon production of about 4 mm/s taking into account the significant damage of the target after each shot. This would cause a pressure rise in the vacuum chamber up to $7*10^{-5}$ mbar. A number of technical limitations related to the vacuum system operation did not allowed to connect the TERESA station to the laser beam transport at this pressure. Under such conditions, only a short sequences of two or three shots was feasible at 1 Hz repetition rate. The investigation of proton energy fluctuation was made at lower repetition rate since this allowed to reduce the ribbon velocity and to keep the chamber pressure below the allowed value. **Figure 7** shows the average proton energy spectrum obtained for the 100-μm thick hydrogen ribbon accelerated into the forward direction by ~1 J laser pulse with a repetition rate 0.1 Hz. The distribution shows an exponential shape, which is typical for the TNSA acceleration mechanism. The cut-off proton energy reaches ~1.5 MeV.

Owing to the wiggling of the ribbon position, the proton energy distribution varies from shot to shot. The fluctuation of the proton energy distribution is presented in **Figure 8**. It shows the energy distribution of 18 consecutive shots measured in one sequence with the amplitude of the signals represented in color. The energy of the ion signal ranges between 0.1 and 2 MeV. Considering a typical proton emission cone to contain within an angle of ~30°, as measured in previous experiments [22], the laser-to-ion energy conversion efficiency was estimated to be around 3%, which is a typical value for the TNSA regime. The proton spectra show clear oscillations in terms of cutoff energy. Protons with cut-off energies varying from 0.7 to 1.5 MeV are

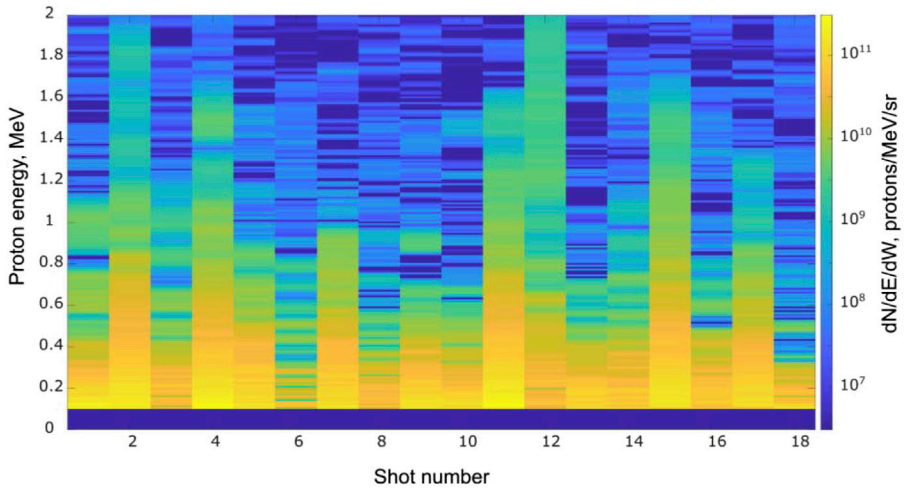

FIGURE 8 | Proton energy distributions recorded for 18 consecutive shots.

generated in about 45% of the laser shots. This result is in agreement with observed positioning jitter of the ribbon.

CONCLUSION

We presented and discussed the capability of the ELISE solid hydrogen target delivery system to operate at Hz-level repetition rate at relativistic laser intensities (~10^{19} W/cm^2). The second generation of ELISE based on cryogen-free pulse-tube system was used at the TERESA facility with the L3-HAPLS laser at ELI Beamlines. The behavior of the target during the extrusion suitable for Hz-level repetition rate was studied. The measured stability of the target position along the laser propagation axis shows that for 45% of the total shots the target remains within the Rayleigh range of the laser waist and the stability tends to improve with increasing the extrusion velocity. Laser pulses with energy higher than 1 J (~5*10^{19} W/cm^2 intensity) evaporated the target surroundings and, after the shot, the damage extended to a few mm from the center of the focal spot. This required to increase the ribbon velocity for a fast target refreshing. A proof-of-principle demonstration of proton acceleration at high repetition rate was reported (0.1 Hz at ~1 J). The observed cutoff energy of the generated proton beams oscillated from 0.7 to 1.5 MeV. Details of the TERESA-ELISE vacuum operation with a continuously extruded ribbon are discussed, and a possible improvement of the vacuum system is suggested. The stability of the target along the laser propagation axis in terms of shot-to-shot fluctuations is also a subject of further improvement. The presented results are of general interest for the community operating laser-driven secondary sources (protons, ions, neutrons, etc.) at high repetition rate (1–10 Hz) using 10–100 TW class lasers systems.

DATA AVAILABILITY STATEMENT

The original contributions presented in the study are included in the article/Supplementary Material, further inquiries can be directed to the corresponding author.

AUTHOR CONTRIBUTIONS

Investigation, all authors; Writing original draft preparation, TC, AV, and DM.

FUNDING

This work has been supported by the project Advanced research using high-intensity laser-produced photons and particles (CZ.02.1.01/0.0/0.0/16_019/0000789) from European Regional Development Fund (ADONIS) and IMPULSE project by the European Union Framework Program for Research and Innovation Horizon 2020 under grant agreement No 871161.

ACKNOWLEDGMENTS

The authors gratefully acknowledge Thomas Goy, Pavel Korous, Martin Laub, Lukas Brabec, Martin Bucka, Petr Voboril, Marek Rajdl, Petr Kemeny, Lubos Nims, Martin Tuma, Pavel Bakule, Birgit Plotzeneder, Antonin Fajstavr, Jakub Cerny, Milan Berta, Vojitech Gaman, Radek Horalek, Petr Mazurek, Roman Kuratko, Libor Tirol, Veronika Olsovcova, Roberto Versaci, David Horvath, Marek Bizdra, Roman Trunecek, Vojtech Stransky, Hana Manaskova, Petr Prochazka and Jaroslav Kaspar for the valuable technical support provided.

REFERENCES

1. Toth C, Evans D, Gonsalves AJ, Kirkpatrick M, Magana A, Mannino G, et al. *Transition of the BELLA PW Laser System towards a Collaborative Research Facility in Laser Plasma Science*. AIP Conf Proc (2017). doi:10.1063/1.4975918
2. Roso L. High Repetition Rate Petawatt Lasers. *EPJ Web of Conferences* (2018) 167:01001. doi:10.1051/epjconf/201816701001
3. Sistrunk E, Spinka T, Bayramian A, Betts S, Bopp R, Buck S, et al. All Diode-Pumped, High-Repetition-Rate Advanced Petawatt Laser System (HAPLS). In: Conference on Lasers and Electro-Optics, 2. (Washington, DC: OSA) (2017), STh1L.2. doi:10.1364/CLEO_SI.2017.STh1L.2
4. Navratil P, Slezak O, Pilar J, Ertel KG, Hanus M, Banerjee S, et al. Characterization of Bivoj/DiPOLE 100: HiLASE 100-J/10-Hz Diode Pumped Solid State Laser. In: Clarkson Shori, editors. *Solid State Lasers XXVII: Technology and Devices*. Bellingham, WA: SPIE (2018). p. 33. doi:10.1117/12.2290290
5. Kar S, Kakolee KF, Qiao B, Macchi A, Cerchez M, Doria D, et al. Ion Acceleration in Multispecies Targets Driven by Intense Laser Radiation Pressure. *Phys Rev Lett* (2012) 109:185006. doi:10.1103/PhysRevLett.109.185006
6. Macchi A, Borghesi M, Passoni M. Ion Acceleration by Superintense Laser-Plasma Interaction. *Rev Mod Phys* (2013) 85:751–93. doi:10.1103/RevModPhys.85.751
7. Bulanov SV, Esirkepov TZ, Khoroshkov VS, Kuznetsov AV, Pegoraro F. Oncological Hadrontherapy with Laser Ion Accelerators. *Phys Lett A* (2002) 299:240–7. doi:10.1016/S0375-9601(02)00521-2
8. Linz U, Alonso J. Laser-driven Ion Accelerators for Tumor Therapy Revisited. *Phys Rev Accel Beams* (2016) 19:124802. doi:10.1103/PhysRevAccelBeams.19.124802
9. Chaudhary P, Milluzzo G, Ahmed H, Odlozilik B, McMurray A, Prise KM, et al. Radiobiology Experiments with Ultra-high Dose Rate Laser-Driven Protons: Methodology and State-Of-The-Art. *Front Phys* (2021) 9:1–12. doi:10.3389/fphy.2021.624963
10. Disdier L, Garçonnet J-P, Malka G, Miquel J-L. Fast Neutron Emission from a High-Energy Ion Beam Produced by a High-Intensity Subpicosecond Laser Pulse. *Phys Rev Lett* (1999) 82:1454–7. doi:10.1103/PhysRevLett.82.1454
11. Norreys PA, Fews AP, Beg FN, Bell AR, Dangor AE, Lee P, et al. Neutron Production from Picosecond Laser Irradiation of Deuterated Targets at Intensities of. *Plasma Phys Control Fusion* (1998) 40:175–82. doi:10.1088/0741-3335/40/2/001
12. Klir D, Krasa J, Cikhardt J, Dudzak R, Krousky E, Pfeifer M, et al. Efficient Neutron Production from Sub-nanosecond Laser Pulse Accelerating Deuterons on Target Front Side. *Phys Plasmas* (2015) 22:093117. doi:10.1063/1.4931460
13. Prencipe I, Fuchs J, Pascarelli S, Schumacher DW, Stephens RB, Alexander NB, et al. Targets for High Repetition Rate Laser Facilities: Needs, Challenges and Perspectives. *High Pow Laser Sci Eng* (2017) 5: e17. doi:10.1017/hpl.2017.18
14. Chagovets T, Stanček S, Giuffrida L, Velyhan A, Tryus M, Grepl F, et al. Automation of Target Delivery and Diagnostic Systems for High Repetition Rate Laser-Plasma Acceleration. *Appl Sci* (2021) 11:1680. doi:10.3390/app11041680
15. George KM, Morrison JT, Feister S, Ngirmang GK, Smith JR, Klim AJ, et al. High-repetition-rate (kHz) Targets and Optics from Liquid Microjets for High-Intensity Laser-Plasma Interactions. *High Pow Laser Sci Eng* (2019) 7: e50. doi:10.1017/hpl.2019.35
16. Morrison JT, Feister S, Frische KD, Austin DR, Ngirmang GK, Murphy NR, et al. MeV Proton Acceleration at kHz Repetition Rate from Ultra-intense Laser Liquid Interaction. *New J Phys* (2018) 20:022001. doi:10.1088/1367-2630/aaa8d1
17. Levato T, Goncalves LV, Giannini V. Laser-Plasma Accelerated Protons: Energy Increase in Gas-Mixtures Using High Mass Number Atomic Species. *Fluids* (2019) 4:150. doi:10.3390/fluids4030150
18. Semushin S, Malka V. High Density Gas Jet Nozzle Design for Laser Target Production. *Rev Scientific Instr* (2001) 72:2961–5. doi:10.1063/1.1380393
19. Poole PL, Andereck CD, Schumacher DW, Daskalova RL, Feister S, George KM, et al. Liquid crystal Films as On-Demand, Variable Thickness (50-5000 Nm) Targets for Intense Lasers. *Phys Plasmas* (2014) 21:063109. doi:10.1063/1.4885100
20. Poole PL, Obst L, Cochran GE, Metzkes J, Schlenvoigt H-P, Prencipe I, et al. Laser-driven Ion Acceleration via Target normal Sheath Acceleration in the Relativistic Transparency Regime. *New J Phys* (2018) 20:013019. doi:10.1088/1367-2630/aa9d47
21. Kim JB, Göde S, Glenzer SH. Development of a Cryogenic Hydrogen Microjet for High-Intensity, High-Repetition Rate Experiments. *Rev Sci Instrum* (2016) 87:11E328. doi:10.1063/1.4961089
22. Polz J, Robinson APL, Kalinin A, Becker GA, Fraga RAC, Hellwing M, et al. Efficient Laser-Driven Proton Acceleration from a Cryogenic Solid Hydrogen Target. *Sci Rep* (2019) 9:16534. doi:10.1038/s41598-019-52919-7
23. Garcia S, Chatain D, Perin JP. Continuous Production of a Thin Ribbon of Solid Hydrogen. *Laser Part Beams* (2014) 32:569–75. doi:10.1017/S0263034614000524
24. Margarone D, Velyhan A, Dostal J, Ullschmied J, Perin JP, Chatain D, et al. Proton Acceleration Driven by a Nanosecond Laser from a Cryogenic Thin Solid-Hydrogen Ribbon. *Phys Rev X* (2016) 6:041030. doi:10.1103/PhysRevX.6.041030
25. Kraft SD, Obst L, Metzkes-Ng J, Schlenvoigt H-P, Zeil K, Michaux S, et al. First Demonstration of Multi-MeV Proton Acceleration from a Cryogenic Hydrogen Ribbon Target. *Plasma Phys Control Fusion* (2018) 60:044010. doi:10.1088/1361-6587/aaae38
26. Margarone D, Cirrone G, Cuttone G, Amico A, Andò L, Borghesi M, et al. ELIMAIA: A Laser-Driven Ion Accelerator for Multidisciplinary Applications. *QuBS* (2018) 2:8. doi:10.3390/qubs2020008
27. Tryus M, Grepl F, Chagovets T, Velyhan A, Giuffrida L, Stancek S, et al. TERESA Target Area at ELI Beamlines. *QuBS* (2020) 4:37. doi:10.3390/qubs4040037
28. Prasad R, Doria D, Ter-Avetisyan S, Foster PS, Quinn KE, Romagnani L, et al. Calibration of Thomson Parabola-MCP Assembly for Multi-MeV Ion Spectroscopy. *Nucl Instr Methods Phys Res Section A: Acc Spectrometers, Detectors Associated Equipment* (2010) 623:712–5. doi:10.1016/j.nima.2010.02.078
29. Knudsen M. *The Kinetic Theory of Gases*. London: Metheun (1934).
30. Ekin J. *Experimental Techniques for Low-Temperature Measurements*. USA: Oxford UniversityPress (2006).doi:10.1093/acprof:oso/9780198570547.001.0001
31. Frost W. *Heat Transfer at Low Temperatures*. New York: Plenum Press (1975).

Conflict of Interest: The authors declare that the research was conducted in the absence of any commercial or financial relationships that could be construed as a potential conflict of interest.

Publisher's Note: All claims expressed in this article are solely those of the authors and do not necessarily represent those of their affiliated organizations, or those of the publisher, the editors and the reviewers. Any product that may be evaluated in this article, or claim that may be made by its manufacturer, is not guaranteed or endorsed by the publisher.